Understanding the impact of the central atom on the ionic liquid behavior: Phosphonium vs ammonium cations

Pedro J. Carvalho, Sónia P. M. Ventura, Marta L. S. Batista, Bernd Schröder, Fernando Gonçalves, José Esperança, Fabrice Mutelet, and João A. P. Coutinho'

Citation: The Journal of Chemical Physics **140**, 064505 (2014); doi: 10.1063/1.4864182
View online: http://dx.doi.org/10.1063/1.4864182
View Table of Contents: http://aip.scitation.org/toc/jcp/140/6
Published by the American Institute of Physics

Understanding the impact of the central atom on the ionic liquid behavior: Phosphonium vs ammonium cations

Pedro J. Carvalho,[1] Sónia P. M. Ventura,[1] Marta L. S. Batista,[1] Bernd Schröder,[1] Fernando Gonçalves,[2] José Esperança,[3] Fabrice Mutelet,[4] and João A. P. Coutinho[1,a)]
[1]*CICECO, Departamento de Química, Universidade de Aveiro, 3810-193 Aveiro, Portugal*
[2]*Departamento de Biologia e CESAM (Centro de Estudos do Ambiente e do Mar), Universidade de Aveiro, 3810-193 Aveiro, Portugal*
[3]*Instituto de Tecnologia Química e Biológica, Universidade Nova de Lisboa, 2780-901 Oeiras, Portugal*
[4]*Laboratoire Réactions et Génie des Procédés, CNRS (UPR3349), Nancy-Université, 1 rue Grandville, BP 20451 54001 Nancy, France*

(Received 3 October 2013; accepted 23 January 2014; published online 12 February 2014)

The influence of the cation's central atom in the behavior of pairs of ammonium- and phosphonium-based ionic liquids was investigated through the measurement of densities, viscosities, melting temperatures, activity coefficients at infinite dilution, refractive indices, and toxicity against *Vibrio fischeri*. All the properties investigated are affected by the cation's central atom nature, with ammonium-based ionic liquids presenting higher densities, viscosities, melting temperatures, and enthalpies. Activity coefficients at infinite dilution show the ammonium-based ionic liquids to present slightly higher infinite dilution activity coefficients for non-polar solvents, becoming slightly lower for polar solvents, suggesting that the ammonium-based ionic liquids present somewhat higher polarities. In good agreement these compounds present lower toxicities than the phosphonium congeners. To explain this behavior quantum chemical gas phase DFT calculations were performed on isolated ion pairs at the BP-TZVP level of theory. Electronic density results were used to derive electrostatic potentials of the identified minimum conformers. Electrostatic potential-derived CHelpG and Natural Population Analysis charges show the **P** atom of the tetraalkylphosphonium-based ionic liquids cation to be more positively charged than the **N** atom in the tetraalkylammonium-based analogous IL cation, and a noticeable charge delocalization occurring in the tetraalkylammonium cation, when compared with the respective phosphonium congener. It is argued that this charge delocalization is responsible for the enhanced polarity observed on the ammonium based ionic liquids explaining the changes in the thermophysical properties observed. © *2014 AIP Publishing LLC*. [http://dx.doi.org/10.1063/1.4864182]

INTRODUCTION

Ionic liquids (ILs) are composed of ions, and as a result, there are a large number of potential compounds to be synthesized by simple structural rearrangements. ILs may be either inert, acting only as solvents, or can be designed to actively participate in a large range of chemical reactions. These ionic compounds have often been considered as "*green solvents*"[1] because of their negligible vapor pressures and, in many cases, low flammability, when compared with common organic solvents. Moreover, the ionic nature of ILs is the main characteristic responsible for some of their most outstanding properties, namely a high ionic conductivity, high thermal and chemical stability, and enhanced solvation ability for a large array of compounds.[2,3] At the same time, the combination of different ions, sustained by a wide chemical diversity, allows the tailoring of their properties, making them *quasi* specific fluids for a particular application, thus "*designer solvents.*" Nonetheless and despite the large number of works outing ionic liquids as "*designer solvents,*" the number of studies dealing with their structural design, besides the simple combination of cations and anions, is, at this point, surprisingly scarce.

This work is part of a series of systematic studies aimed at developing the knowledge inherent to the ILs' structure/behavior duality and ultimately create general rules for the ILs design. Specific heuristics have been previously proposed covering the ILs' structural characteristics, namely the alkyl chain length and isomerism and the presence/absence of the aromaticity effect in a large range of physical, chemical, and biological properties.[4–7] It aims at understanding the impact in the ILs thermodynamic, thermophysical, and biological properties promoted by the simple substitution of a phosphorous by a nitrogen atom on the cation's core. In contrast to the ion substitution studies, the atom substitution, of the constituent ions, has been object of a limited number of studies.[8–13] Shirota and Castner[11] reported that the substitution of carbon by silicon in the neopentyl group at the imidazolium cation (1-methyl-3-neopentylimidazolium ($[Cmim]^+$) *vs* 1-methyl-3-trimethylsilylmethylimidazolium ($[Simim]^+$)) leads to a substantial reduction of viscosity. On the anionic side, the heavy atom substitution in a series of $[XF_6]^-$ anions (X = P, As, or Sb) in 1-butyl-3-methylimidazolium

a)Author to whom correspondence should be addressed. Electronic mail: jcoutinho@ua.pt. Tel.: +351-234-370200. Fax: +351-234-370084.

($[C_4mim]^+$)-based ILs also affects the viscosity: 290 cP for $[C_4mim][PF_6]$, 228 cP for $[C_4mim][AsF_6]$, and 134 cP for $[C_4mim][SbF_6]$.[12] In addition to studies with aromatic cation-based ILs, reductions in the viscosities of ILs with heavier atoms in the same position were also reported for non-aromatic cation-based ILs.[8,10,13,14]

Tsunashima and co-workers[8,9] were the first to compare the behavior of pairs of $[NTf_2]^-$ anion-based ammonium and phosphonium ionic liquids investigating the differences upon viscosities, conductivities, and thermal stability. Contrary to most neutral molecular liquids, where the substitution of a constituent atom by a heavier atom leads to a viscosity increase, the authors[8] reported lower viscosities and higher conductivities for the phosphonium, when compared to those of corresponding ammonium ILs. Furthermore, in a later study[9] the authors reported higher thermal stability for benzyl-substituted phosphonium, compared to the corresponding benzyl-substituted ammonium compounds. Shirota *et al.*[10] suggested that the unexpected properties change, achieved by the heavy atom substitution in the ILs cation central atom, result from weaker interionic interactions, due to the ionic volume increase, and that this substitution has an impact on bulk properties (i.e., density and viscosity) but not on surface properties (i.e., surface tension). This is further confirmed by the results reported by Lee *et al.*[14] using NOE 2D NMR.

Aiming at extending these studies to other pairs of ammonium/phosphonium ionic liquids with variable chain lengths and different anions than those previously investigated, four pairs of ammonium/phosphonium ILs, only distinguishable by the cation's central atom, were studied through the determination of the properties: (i) density, viscosity, and refractive indices for the compounds in the liquid state and melting points for the solid ILs, (ii) infinite dilution activity coefficients on a large set of solvents, (iii) ecotoxicity investigated by Microtox® assays. To try to provide an explanation for the differences in behavior observed, quantum chemical gas phase DFT calculations were performed on isolated ion pairs at the BP-TZVP level of theory for some of the IL pairs investigated.

MATERIALS AND METHODS

Materials

This work was developed using eight ILs based on the quaternary ammonium and phosphonium cations, namely, tributylhexylammonium bis(trifluoromethylsulfonyl)imide, $[N_{4,4,4,6}][NTf_2]$, tributylhexylphosphonium bis(trifluoromethylsulfonyl)imide, $[P_{4,4,4,6}][NTf_2]$, tributylhexylammonium hexafluorophosphate, $[N_{4,4,4,6}][PF_6]$, tetrabutylammonium hexafluorophosphate, $[N_{4,4,4,4}][PF_6]$, tributylhexylphosphonium hexafluorophosphate, $[P_{4,4,4,6}][PF_6]$, tetrabutylphosphonium hexafluorophosphate, $[P_{4,4,4,4}][PF_6]$, trioctylmethylammonium bis(trifluoromethylsulfonyl)imide, $[N_{8,8,8,1}][NTf_2]$, and trioctylmethylphosphonium bis(trifluoromethylsulfonyl)imide, $[P_{8,8,8,1}][NTf_2]$. The chemical structures, purity, and supplier are displayed in Figure 1.

To reduce the water and volatile compounds content to negligible values, ILs individual samples were dried under moderate vacuum and temperature, for a minimum of 48 h. After this procedure, the purity of each IL was confirmed by ^1H, ^{13}C, and ^{19}F NMR and shown to be better than 98% for all the compounds investigated. The water concentration of dried ILs was determined through Karl Fisher titration and was less than 3×10^{-4} mass fraction. The water used was ultra-pure water, double distilled, passed by a reverse osmosis system and further treated with a Milli-Q plus 185 water purification apparatus.

Methods

Density, viscosity, and melting points

Viscosity and density data were measured for the ILs $[N_{4,4,4,6}][NTf_2]$, $[P_{4,4,4,6}][NTf_2]$, $[N_{8,8,8,1}][NTf_2]$, and $[P_{8,8,8,1}][NTf_2]$ using an automated SVM 3000 Anton Paar rotational Stabinger viscometer-densimeter in the temperature range from 283.15 to 373.15 K, within an uncertainty of ±0.02 K and at atmospheric pressure. The relative uncertainty of the dynamic viscosity obtained is ±0.35%, while the absolute uncertainty in density is $\pm 5 \times 10^{-4}$ g cm^{-3}. Further details about the equipment and method can be found in Refs. 15 and 16.

The ILs $[N_{4,4,4,6}][PF_6]$ and $[P_{4,4,4,6}][PF_6]$ are not liquid within the temperature range available for the density and viscosity measurements, therefore, their density and viscosity were not collected.

The melting points and glass transition temperatures of the ILs investigated were determined through a DSC (Diamond Differential Scanning Calorimetry) Perkin Elmer equipment, using a Universal Thermal Analyzer DSC Q200 V23.12.

The analytical procedure included a cooling ramp down to 183.15 K and a heating ramp up to 733.15 K at a rate of 0.167 K s^{-1}. The ILs were submitted to three cycles of cooling and heating with a constant nitrogen flow of 0.833 cm^3 s^{-1}, supplied to the DSC cell in order to avoid condensation of water at the lower temperatures. At least two independent runs were performed for each compound.

Refractive index

Refractive indices (n_D), at 589.3 nm, were measured for the ILs $[N_{4,4,4,6}][NTf_2]$, $[P_{4,4,4,6}][NTf_2]$, $[N_{8,8,8,1}][NTf_2]$, and $[P_{8,8,8,1}][NTf_2]$ using an automated Abbemat 500 Anton Paar refractometer, at 298.15, 323.15, and 348.15 K and atmospheric pressure. The instrument uses reflected light to measure the refractive index, where the sample on top of the measuring prism is irradiated from different angles by a LED. The maximum deviation in temperature is ±0.01 K and the maximum uncertainty in the refractive index measurements is ±0.00002, respectively. The derived molar refractions, R_m, free volumes, f_m, and polarizabilities were determined, as well as the following:[17–19]

$$\frac{\alpha_0}{4\pi\varepsilon_0} = \left(\frac{n_D^2 - 1}{n_D^2 + 2}\right)\frac{3M_r}{4\pi\rho N_A}, \quad (1)$$

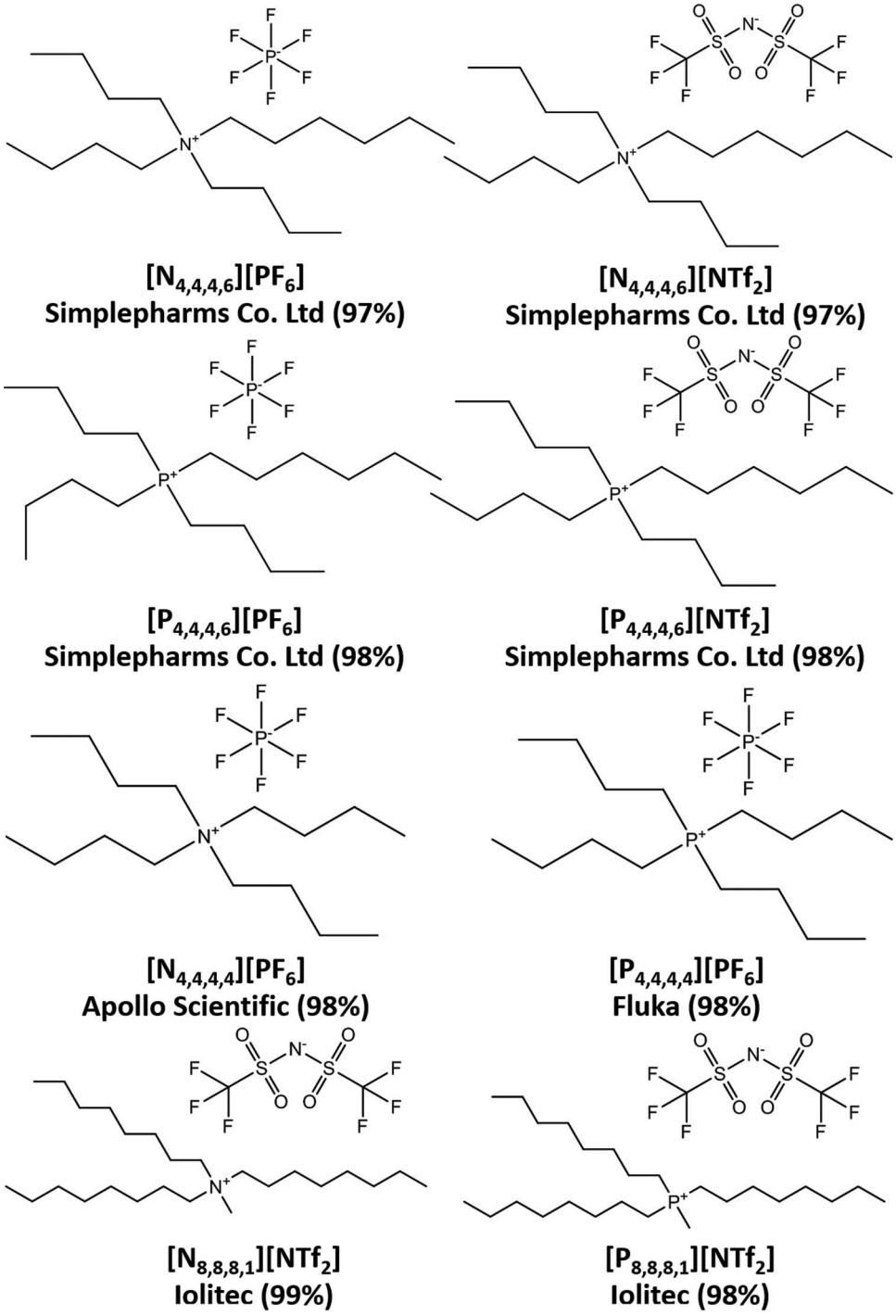

FIG. 1. Chemical structure, abbreviations, purity, and supplier of all ILs investigated.

where α_0 is the electronic polarizability, ε_0 is the vacuum permittivity, ρ is the compound's density, M_r is the molecular weight, and N_A is the Avogadro number

$$R_m = \frac{N_A \alpha_0}{3\varepsilon_0} = \left(\frac{n^2 - 1}{n^2 + 1}\right) V_m, \tag{2}$$

where V_m is the molar volume

$$f_m = V_m - R_m. \tag{3}$$

Activity coefficients at infinite dilution

Inverse chromatography experiments were carried out using a Varian CP-3800 gas chromatograph equipped with a heated on-column injector and a flame ionization detector. The injector and detector temperatures were kept at 523 K during all experiments. The helium flow rate was adjusted to obtain adequate retention times. Methane was used to determine the column hold-up time. A more detailed description about the equipment

and method can be found in the supplementary material.[43]

The retention data garnered by inverse chromatography experiments were used to calculate partition coefficients of the numerous solutes in the different ILs. The standardized retention volume, V_N, was calculated following the relationship[20,21]

$$V_N = J \cdot U_0 t'_R \frac{T_{col}}{T_{rt}} \left(1 - \frac{P_{ow}}{P_0}\right). \quad (4)$$

The adjusted retention time, t'_R, was taken as the difference between the retention time of a particular solute and that of methane, T_{col} is the column temperature, U_o is the flow rate of the carrier gas measured at room temperature (T_{rt}), P_{ow} is the vapor pressure of water at T_{rt}, and P_o is the outlet pressures. The factor J in Eq. (4) corrects for the influence of the pressure drop along the column and is given through the relation[20,21]

$$J = \frac{3}{2} \frac{\left[\left(\frac{P_i}{P_0}\right)^2 - 1\right]}{\left[\left(\frac{P_i}{P_0}\right)^3 - 1\right]}, \quad (5)$$

where P_i is the inlet pressure.

Activity coefficients at infinite dilution for solute 1 in each IL, $\gamma^{\infty}_{i,IL}$, were calculated with the following expression:[20,21]

$$\ln \gamma^{\infty}_{1,IL} = \ln\left(\frac{n_2 R \cdot T}{V_N P^0_i}\right) - P^0_1 \frac{B_{11} - V^0_1}{R \cdot T} + \frac{2B_{13} - V^{\infty}_i}{R \cdot T} J \cdot P_0, \quad (6)$$

where n_2 is the number of moles of stationary phase component within the column, R is the ideal gas constant, T is the oven temperature, B_{11} is the second virial coefficient of the solute in the gaseous state at temperature T, B_{13} is the mutual virial coefficient between solute 1 and the carrier gas (helium, denoted by "3"), and P^0_1 is the probe's vapor pressure at temperature T. The values of P^0_1 result from correlated experimental data. The molar volume of the solute, V^0_1 was determined from experimental densities and the partial molar volumes of the solutes at infinite dilution, V^{∞}_i, were assumed to be equal to V^0_1. The values required for the calculation of these parameters were taken from previous works.[22]

Microtox® toxicity tests

The Microtox® test[23] was used to evaluate the inhibition of the luminescence in the bacteria *Vibrio fischeri* using a procedure detailed in Refs. 7 and 24. The bacterium was exposed to a range of diluted aqueous solutions (typically from 0% to 81.9%) of each IL, where 100% of IL corresponds to the known concentration of a stock solution previously prepared. After 5, 15, and 30 min of exposure to the IL, the light output of the luminescent bacteria is measured and compared with the light output of a blank control sample, allowing the estimation of the corresponding 5, 15 and 30 min-EC_{50} values through Microtox® Omni™ Software version 4.1.[25]

Partial charges and charge delocalization

In quantum chemical gas phase calculations, geometries, and atom charges of the isolated ion pairs were optimized using the TZVP basis set and non-local BP exchange/correlation functional as implemented in Gaussian 03 Rev D.02.[26] After independently optimizing the constituting ions, different initial guess conformations for the two isolated ion pairs were prepared by matching the most positive areas of the cation with the most negative areas in the anion. Then, initial geometries were optimized; vibrational analysis on the obtained structures confirmed the presence of true minima on the potential energy surface. On the obtained minima, atomic charges of the six different ionic pairs were retrieved by Mulliken population analysis[27] as well as electrostatic surface potential (ESP) fits, using the CHelpG algorithm[28] to electron densities obtained at the BP/TZVP level.

RESULTS AND DISCUSSION

Density, viscosity, melting points, and refractive indices

Viscosity and density measurements were carried out in the temperature range of (283.15–373.15) K at atmospheric pressure, as depicted in Figure 2 and reported in Table I. The change of a **P** (Ar = 30.9738) for a **N** (Ar = 14.006) leads to a surprising increase in both the density and viscosity of the IL pairs. Inverting the effect of the addition of a heavier atom, the densities of the ammonium are higher than those of phosphonium, and this effect is even more noticeable on the viscosities. Although it could be expected that the introduction of a heavier atom would increase the densities and viscosities, as commonly observed, or that the large cation's alkyl chains used in this study would shield the central atom and therefore smooth or even remove its influence on the interactions, and ultimately on the properties of the IL, the viscosity and density results show that even surrounded by large alkyl chains, the cation's central atom still has an important impact on these basic thermophysical properties. The two pairs here reported present the same behavior previously observed by Tsunashima *et al.*[8] and Shirota *et al.*[10] Tsunashima *et al.*[8] reported a ^{1}H NMR chemical shift towards a high magnetic field, of the ammonium CH_2 groups adjacent to the cationic center compared to the corresponding phosphonium. The authors suggested that the shifts observed are attributed to relatively high electron density of the protons in the phosphonium cations and that this electron density increase leads to lower acidity and lower electrostatic interactions of the phosphonium ILs and therefore, to a density decrease.[8] Shirota *et al.*,[10] supporting the work of Tsunashima and co-workers,[8] stated that the substitution of the ILs cation central atom, with a heavier atom, leads to weaker interionic interactions due to the ionic volume increase. Furthermore, according to the authors this substitution is more relevant on bulk properties, such as viscosity and density, and almost negligible on surface properties, such as surface tension.

Their melting points and glass transition temperatures were measured and are reported in Table II. Similarly to what was observed for the density and viscosity, the change of the

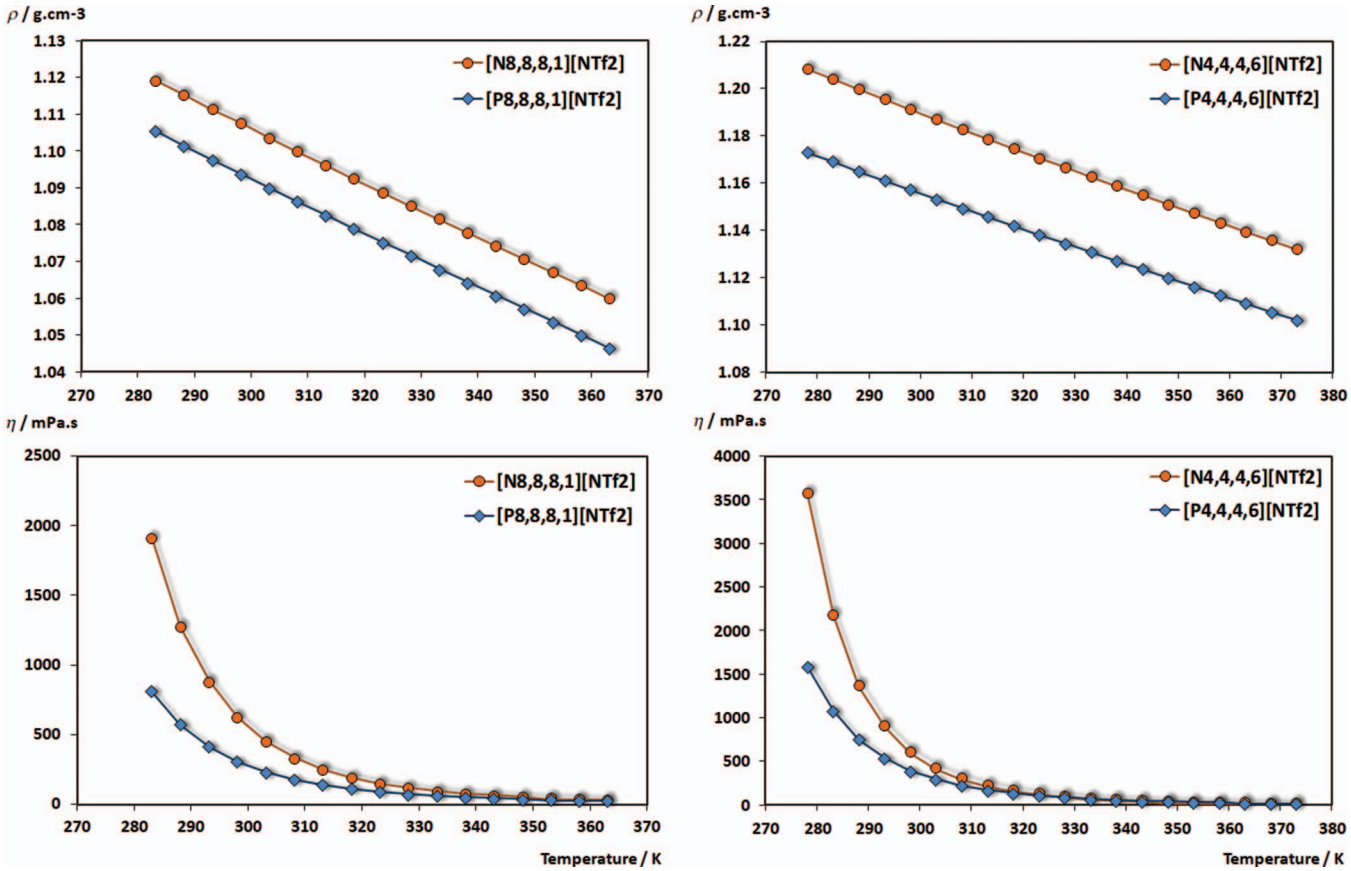

FIG. 2. Density (top) and viscosity (bottom) for the studied [NTf_2] anion-based ILs. The solid curves are guides for the eyes.

TABLE I. Experimental densities (ρ), viscosities (μ), and molar volumes (V_m).

	ρ (g cm^{-3})	μ (mPa s)	Vm (cm^3 mol^{-1})	ρ (g cm^{-3})	μ (mPa s)	Vm (cm^3 mol^{-1})	ρ (g cm^{-3})	μ (mPa s)	Vm (cm^3 mol^{-1})	ρ (g cm^{-3})	μ (mPa s)	Vm (cm^3 mol^{-1})
T (K)	[$N_{8,8,8,1}$][NTf_2]			[$P_{8,8,8,1}$][NTf_2]			[$N_{4,4,4,6}$][NTf_2]			[$P_{4,4,4,6}$][NTf_2]		
278.15							1.2081	3573.70	455.81	1.1729	1589.3	483.95
283.15	1.1191	1905.20	580.69	1.1056	806.54	603.13	1.2039	2173.00	457.40	1.1690	1077.8	485.57
288.15	1.1152	1272.10	582.72	1.1016	569.19	605.32	1.1996	1374.10	459.04	1.1650	751.99	487.24
293.15	1.1113	877.56	584.76	1.0977	411.22	607.47	1.1954	910.46	460.65	1.1609	542.14	488.96
298.15	1.1075	619.64	586.77	1.0938	303.04	609.63	1.1911	611.32	462.31	1.1570	391.90	490.61
303.15	1.1035	446.75	588.90	1.0900	227.45	611.76	1.1868	426.67	463.99	1.1531	291.62	492.26
308.15	1.0997	328.50	590.93	1.0863	173.60	613.84	1.1827	305.82	465.60	1.1493	220.77	493.89
313.15	1.0960	246.02	592.93	1.0826	134.59	615.94	1.1786	225.69	467.22	1.1455	170.65	495.53
318.15	1.0923	187.39	594.94	1.0789	105.87	618.05	1.1746	168.22	468.81	1.1418	132.53	497.14
323.15	1.0886	145.00	596.96	1.0753	84.42	620.12	1.1706	128.62	470.41	1.1380	104.88	498.80
328.15	1.0850	113.88	598.94	1.0716	68.18	622.26	1.1666	100.02	472.02	1.1344	84.037	500.38
333.15	1.0814	90.68	600.93	1.0679	55.73	624.42	1.1627	79.08	473.61	1.1307	68.281	502.02
33815	1.0778	73.14	602.94	1.0643	46.03	626.53	1.1588	63.19	475.20	1.1270	55.795	503.66
343.15	1.0742	59.69	604.96	1.0607	38.41	628.66	1.1549	51.30	476.81	1.1234	46.185	505.28
348.15	1.0706	49.26	607.00	1.0571	32.37	630.80	1.1510	42.09	478.42	1.1197	38.566	506.95
353.15	1.0670	41.07	609.04	1.0535	27.51	632.95	1.1472	34.98	480.01	1.1161	32.527	508.58
358.15	1.0635	34.57	611.05	1.0499	23.58	635.12	1.1433	29.30	481.64	1.1125	27.559	510.23
363.15	1.0599	29.38	613.12	1.0464	20.38	637.25	1.1395	24.83	483.25	1.1089	23.562	511.89
368.15							1.1357	21.18	484.87	1.1053	20.286	513.55
373.15							1.1320	18.27	486.45	1.1018	17.633	515.18

TABLE II. Melting temperature (T_m), enthalpy (ΔH_{fus}), and entropy (ΔS_{fus}) of the studied ILs.

	$T_m \pm \sigma$ (K)	$\Delta H_{fus} \pm \sigma$ (kJ mol^{-1})	$\Delta S_{fus} \pm \sigma$ (kJ mol^{-1} K^{-1})
$[P_{4,4,4,6}][PF_6]$	414.43 ± 0.01	8.50 ± 0.21	0.0205 ± 0.0005
$[N_{4,4,4,6}][PF_6]$	440.17 ± 0.03	9.62 ± 0.22	0.0219 ± 0.0005
$[P_{4,4,4,4}][PF_6]$[a]	498.60 ± 0.03	14.67 ± 0.02	0.0294 ± 0.0001
$[N_{4,4,4,4}][PF_6]$[a]	524.33 ± 0.19	16.41 ± 0.13	0.0313 ± 0.0002
$[P_{4,4,4,6}][NTf_2]$	≪193.15		
$[N_{4,4,4,6}][NTf_2]$	296.85 ± 0.24	44.91 ± 0.76	0.1513 ± 0.003

[a]Neves *et al.*[29] and σ, standard deviation.

cation central atom, a phosphorous by a nitrogen, leads to an increase on both the IL melting temperature and enthalpy. Furthermore, the same behavior was observed for the ILs $[N_{4,4,4,4}][PF_6]$ and $[P_{4,4,4,4}][PF_6]$, recently reported by us.[29] Contrary to Tsunashima and co-workers[8] observations, the liquid ILs studied here follow the same trend, with the change of the cation central atom, a phosphorous by a nitrogen, leading to the increase on both the IL melting temperature and enthalpy.

The experimental refractive indices for the ammonium/phosphonium ILs pairs are listed in Table III at 298.15, 323.15, and 348.15 K along with the derived molar refractions, R_m, and the calculated free volumes, f_m, and polarizabilities, at 298.15 K. The phosphonium-based ILs refractive indices are slightly higher than those of the homologous ammoniums, but the polarizabilities and the free volumes derived molar refractions follow the opposite behavior, the latter in good agreement with the density values measured for these pairs.

Recently, Seki *et al.*[30] evaluated the refractive indices of 17 ILs, as function of temperature, against theoretical polarizabilities obtained through *ab initio* calculations. On the premise that refractive indices are an indication of the dielectric response to an electrical field, induced by electromagnetic waves, and that refractive indices can be considered as the response to electronic polarization as the first order approximation, within an instantaneous time scale, the authors proposed a correlation between the refractive index and the polarizability normalized in terms of the molecular volume.[30]

Following the work of Seki *et al.*[30] the refractive indices of the studied ILs, at 303.15 K, were plotted against the experimental polarizability normalized in terms of the IL molecular volume. As depicted in Figure 3 the correlation proposed by

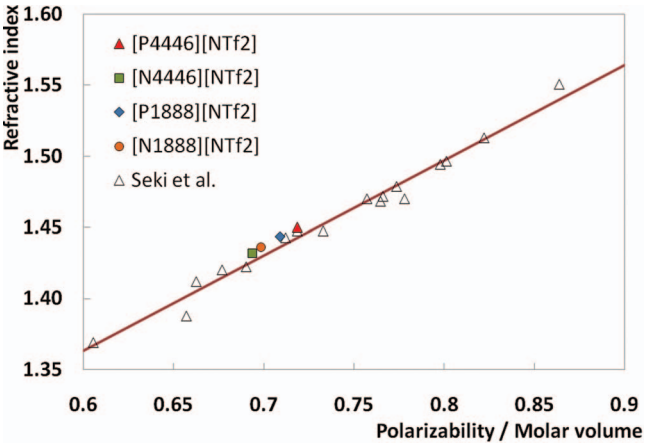

FIG. 3. Relationship between refractive index and polarizability/molecular volume for ILs at 303.15 K. The white triangles and the solid line represent the experimental data and the correlation of Seki *et al.*,[30] respectively.

the authors is able to predict the refractive index from the polarizability and vice versa, within the uncertainty of the correlation.

Activity coefficients at infinite dilution

The experimental activity coefficients at infinite dilution, $\gamma^{\infty}_{1,IL}$, for the ammonium/phosphonium ILs pairs, calculated through Eqs. (4)–(6), are listed in Table IV for 323 K, 333 K, and 343 K, alongside with the solvents solubility parameters, $\delta_{solvent}$, gathered from literature.[31]

In a previous work[32] it was shown that imidazolium-based ionic liquids present an amphiphilic character and are able to interact differently depending on the solute polarity. In fact, this ability to interact either with non-polar, through dispersion forces, and polar solutes/solvents, through dipoles and hydrogen bonding, are the reason behind the enhanced ILs solvation ability. Although, as previously reported for imidazolium-based ILs and other complex molecules,[33–36] this chameleonic behavior is not observed for the ammonium and phosphonium ILs pairs here studied.

The data presented in Table IV shows that, overall, the temperature increase leads to the $\gamma^{\infty}_{1,IL}$ decrease, as commonly observed in literature.[37,38] Moreover, the IL anion is also shown to play a key role on the IL–solvent interactions. In fact $[PF_6]$-based ILs present activity coefficients at infinite dilution two orders of magnitude higher than those of

TABLE III. Refractive indices, isotropic polarizabilities, derived molar refractions (R_m), calculated free volumes (f_m), experimentally and QC derived polarizabilities for the studied ILs at 298.15 K, 323.15 and 348.15 K and atmospheric pressure.

						Polarizability (bohr^3)	
IL	$n_{D(298.15\ K)}$	$n_{D(323.15\ K)}$	$n_{D(348.15\ K)}$	$R_{m,298.15K}$ (cm^3 mol^{-1})	$f_{m,298.15K}$ (cm^3 mol^{-1})	Expt.	BP-TZVP
$[N_{8,8,8,1}][NTf_2]$	1.43794	1.43023	1.42260	153.78	432.09	411.39	426.42
$[P_{8,8,8,1}][NTf_2]$	1.44541	1.43753	1.42971	162.14	446.58	433.76	444.42
$[N_{4,4,4,6}][NTf_2]$	1.43375	1.42614	1.41862	120.34	341.98	321.92	328.36
$[P_{4,4,4,6}][NTf_2]$	1.45156	1.44397	1.43636	132.24	358.37	353.77	346.21

TABLE IV. Experimental activity coefficients at infinite dilution, $\gamma_{1,IL}^{\infty}$ and solubility parameter, $\delta_{sol.}$, of organic compounds in ILs at various temperatures.

		$[N_{4,4,4,6}][PF_6]$ T (K)			$[N_{4,4,4,6}][NTf_2]$ T (K)			$[P_{4,4,4,6}][PF_6]$ T (K)			$[P_{4,4,4,6}][NTf_2]$ T (K)			$[N_{8,8,8,1}][NTf_2]$ T (K)			$[P_{8,8,8,1}][NTf_2]$ T (K)		
Solute	$\delta_{sol.}$	322.25	332.45	342.75	322.25	332.45	342.75	322.75	332.95	342.75	321.55	332.95	343.15	323.15	333.15	343.15	323.15	333.15	343.15
1,4-dioxane	20.5	5.234	5.134	5.179	0.527	0.531	0.529	7.813	7.407	7.045	0.708	0.673	0.661	0.522	0.512	0.513	0.552	0.540	0.535
1-butanol	23.3	10.171	9.613	9.255	1.613	1.454	1.312	11.490	10.276	10.860				1.395	1.176	1.129	1.155	1.330	0.976
1-heptyne					1.416	1.594	1.578				1.503	1.469	1.463	1.037	1.041	1.053	0.953	0.936	0.970
1-hexene	15.1				2.307	2.288	2.247				2.338	2.209	2.143	1.330	1.295	1.281	1.143	1.136	1.136
1-hexyne					1.287	1.281	1.266				1.243	1.209	1.200	0.908	0.895	0.901	0.844	0.840	0.838
1-nitropropane	21.1	32.847	29.414	26.738	0.531	0.528	0.521	23.103	20.912	19.682	0.547	0.563	0.554	0.523	0.874	0.501	0.542	0.519	0.510
1-propanol	24.3	5.022	4.886	4.800	1.427	1.308	1.183	6.749	5.020	5.839	0.557	0.523	0.508	1.360	1.190	1.086	1.151	1.052	0.964
2,2,4-Trimethylpentane														1.999	1.976	1.940	1.688	1.663	1.654
2-butanone	19.0	8.892	8.119	7.040	0.346	0.326	0.299	12.483	10.489	8.922	0.427	0.375	0.341	0.305	0.282	0.261	0.308	0.283	0.262
2-Methyl-1-propanol		9.750	9.400	8.770	1.513	1.372	1.241	12.220	11.299	10.894	0.492	0.511	0.504	1.319	1.181	1.084	1.097	1.000	0.927
2-pentanone		17.938	18.494	17.679	0.419	0.466	0.472	25.536	24.089	21.686	0.547	0.540	0.531	0.373	0.377	0.385	0.369	0.376	0.383
2-propanol	23.5	5.223	5.086	4.919	1.399	1.265	1.154	8.300	6.919	7.115	0.667	0.619	0.603	1.312	1.172	1.080	1.192	1.085	0.999
3-Methylpentane					3.026	2.918	2.787				2.934	2.721	2.620	1.591	1.552	1.513	1.343	1.317	1.307
3-pentanone		17.010	16.770	16.402	0.425	0.434	0.445	25.288	22.312	19.997	0.498	0.489	0.498	0.343	0.350	0.362	0.338	0.351	0.358
Acetonitrile	24.3	1.441	1.866	2.280	0.422	0.378	0.435	1.520	1.515	1.412	0.504	0.515	0.494	0.486	0.425	0.454	0.578	0.549	0.537
Benzene	18.8	10.414	9.291	9.171	0.551	0.568	0.577	8.260	7.863	7.084	0.669	0.640	0.642	0.472	0.469	0.473	0.470	0.463	0.470
Butyraldehyde	18.4	0.199	0.240	0.306	0.487	0.084	0.080				0.428	0.449	0.441						
Chloroforme	19.0	5.781	5.572	5.360	0.482	0.499	0.507	2.739	2.911	3.076	0.260	0.301	0.318	0.404	0.414	0.427	0.370	0.376	0.386
Cycloheptane					5.789	7.879	10.840				5.069	7.060	9.550	2.956	4.139	5.729	2.485	3.502	4.849
Cyclohexane	16.8				2.249	2.106	2.116				2.135	1.977	1.883	1.238	1.201	1.171	1.042	0.999	1.009
Decane	13.5	461.10	429.81	337.72	8.789	8.129	7.641	388.802	406.767	338.666	7.794	6.899	6.544	3.289	3.178	3.111	2.643	2.564	2.523
Dichloromethane	20.3	3.935	4.320	4.720	0.172	0.412	0.422	3.559	3.178	3.014	0.309	0.357	0.367	0.342	0.356	0.369	0.320	0.331	0.343
Diethyl ether	15.1				1.149	1.097	1.133				1.146	1.220	1.044	0.810	0.798	0.801	0.755	0.749	0.748
Di-iso-propyl ether	14.1				2.092	2.077	2.018				1.960	2.079	2.100	1.277	1.266	1.267	1.134	1.122	1.130
Dodecane	16.2	747.76	685.3	648.75				606.251	584.431	575.779									
Ethanol	26.0	2.681	2.618	2.834	0.687	0.758	1.064	12.917	2.167	2.866	0.557	0.518	0.502	1.270	1.133	1.053	1.212	1.098	1.020
Ethylbenzene	18.0	53.440	46.713	44.526	0.989	1.011	1.026	42.707	38.588	35.176	1.155	1.125	1.106	0.681	0.706	0.718	0.676	0.682	0.692
Formaldehyde		0.193	0.219	0.243	0.089	0.097	0.104				0.101	0.117	0.124	0.010	0.086	0.091	0.082	0.087	0.093
Heptane	15.1				4.276	4.077	3.968				4.023	3.670	3.523	1.998	1.952	1.901	0.157	1.638	1.622
Hexane	14.9				3.326	3.199	3.089				3.216	2.491		1.698	1.663	1.630	1.436	1.411	1.398
Methanol	29.6				0.544	0.489	0.671	2.079	1.843	2.514	0.395	0.365	0.332	0.757	0.717	0.665	1.042	0.942	0.880
Methylcyclohexane	15.9				2.819	2.686	2.601				2.612	2.408	2.303	1.424	1.373	1.352	1.131	1.169	1.157
Methylcyclopentane					2.277	2.128	2.182				2.238	2.068	1.932	1.277	1.230	1.201	1.078	1.094	1.046
m-xylene	18.0	60.499	55.849	49.949	1.029	0.647	1.052	46.826	42.276	38.712	1.204	1.170	1.148	0.686	0.694	0.708	0.680	0.673	0.684
Nitromethane	26.0	10.158	9.400	9.283	0.569	0.559	0.536	6.984	6.662	6.238	0.598	0.609	0.580	0.664	0.624	0.599	0.718	0.676	0.644
Nonane	15.6				7.519	7.062	6.668	351.838	323.323	263.141	6.836	6.099	5.772	3.045	2.941	2.868	2.491	2.413	2.361
Octane	15.6				5.409	5.177	4.918				5.003	4.532	4.354	2.358	2.292	2.276	1.954	1.910	1.886
o-xylene	18.0	56.535	50.124	45.588	0.932	0.939	0.960	40.824	36.552	46.946	1.099	1.058	1.055	0.641	0.654	0.670	0.629	0.640	0.653
Propionaldehyde		0.097	0.113	0.148	0.422	0.075	0.124				0.444	0.469	0.463	0.053	0.369	0.365	0.378	0.383	0.374

TABLE IV. (*Continued.*)

		[$N_{4,4,4,6}$][PF_6] T (K)			[$N_{4,4,4,6}$][NTf_2] T (K)			[$P_{4,4,4,6}$][PF_6] T (K)			[$P_{4,4,4,6}$][NTf_2] T (K)			[$N_{8,8,8,1}$][NTf_2] T (K)			[$P_{8,8,8,1}$][NTf_2] T (K)		
Solute	$\delta_{sol.}$	322.25	332.45	342.75	322.25	332.45	342.75	322.75	332.95	342.75	321.55	332.95	343.15	323.15	333.15	343.15	323.15	333.15	343.15
p-xylene	18.0	57.087	51.519	46.276	1.036	1.036	1.041	44.628	41.216	37.028	1.168	1.151	1.119	0.687	0.700	0.707	0.669	0.674	0.679
Pyridine	21.9	1.558	1.730	1.809	0.312	0.303	0.310	13.828	5.857	5.602	0.470	0.450	0.446	0.360	0.359	0.366			
Tetrachloromethane	17.6				1.124	1.125	1.112	12.361	11.985	11.567	0.828	0.901	0.916	0.766	0.767	0.775	0.687	0.690	0.691
Tetradecane		1073.02	1063.46	996.99				897.165	859.374	860.623									
Thiophene	20.1	5.866	5.559	5.462	0.547	0.552	0.515	5.132	5.160	4.717	0.557	0.593	0.590	0.469	0.466	0.469	0.471	0.462	0.462
Toluene	18.2	25.267	22.640	22.139	0.726	0.740	0.755	19.518	17.780	16.607	0.863	0.840	0.836	0.548	0.555	0.567	0.544	0.544	0.556
Tridecane		946.98	881.94	807.39				751.650	731.283	728.042									
Triethylamine	15.1				2.323									1.138	0.776	1.218			
Trifluoroethanol														0.449	0.374	0.398	0.275	0.272	0.269
Undecane		611.61	592.20	476.98	11.127	10.184	9.468	504.459	477.470	451.743	9.824	8.520	7.985		3.735	3.639			2.900

[NTf_2]-based ILs. The ratio between ammonium and phosphonium IL pairs, presented in Figure 4, show that the ammonium-based ILs present somewhat higher activity coefficients at infinite dilution for non-polar solvents, decreasing until becoming slightly lower for polar solvents. Although noticeable for all the ILs pairs studied it is more noticeable for the trioctylmethylphosphonium and trioctylmethylammonium ILs, as depicted in Figure 4. These results suggest a higher polar nature of the ammonium based ionic liquids when compared with the phosphonium based, in agreement with the results for the other thermophysical properties presented before.

Microtox® toxicity tests

The ILs ecotoxicity was investigated using the Microtox® bioassay, a well-known bioluminescence inhibition test assessing on the bacterium *Vibrio fischeri*.

The impact of all the ILs investigated in this work was studied considering various structural features, the length of the alkyl chain substituted in the cation core and the influence of the substitution of the central atom in the cation. Table V shows the EC_{50} results for all ILs at the exposure times of 5, 15, and 30 min. Three exposure times were adopted to assure the total toxic impact of each IL in the organism. Again, the presence of a phosphorous or a nitrogen as the cation's central atom has a significant impact on the IL toxicity. For the same IL pair, the EC_{50} values indicate that the bacterium is more tolerant to the presence of the ammonium than to the phosphonium ILs. The results show that the phosphonium family is more toxic, being this effect independent of the exposure time, anion and alkyl chain lengths (EC_{50}-ammonium > EC_{50}-phosphonium). Moreover, the results of Table V also show that the [NTf_2] anion is the most toxic, which is in close agreement with the literature results.[7,39] Despite the scarce number of studies reporting toxicity data for these non-aromatic and acyclic families, the same tendency here described was also identified in literature.[40] Maginn and co-workers[40] reported the ecotoxicity of tetrabutylammonium bromide, [$N_{4,4,4,4}$][Br], and tetrabutylphosphonium bromide, [$P_{4,4,4,4}$][Br], for the *Vibrio fischeri* bacterium, with the phosphonium-based IL presenting a higher ecotoxicity [$(0.51 < EC_{50} = 0.51 < 0.51)$ mg l^{-1}] in comparison with the ammonium cation [$(1.58 < EC_{50} = 1.86 < 2.18)$ mg l^{-1}].

It is widely accepted in the literature[41,42] that the toxicities of ionic liquids are related with their hydrophobicities. The lower toxicity of the ammonium compounds supports that they present a lower hydrophobic nature (higher polarities) than their corresponding phosphonium counterparts, which is in agreement with the infinite dilution activity coefficients reported.

Partial charges and charge delocalization

To attempt to explain the results o described above, geometries and atom charges of the isolated ion pairs were calculated using the TZVP basis set and non-local BP exchange/correlation function. The

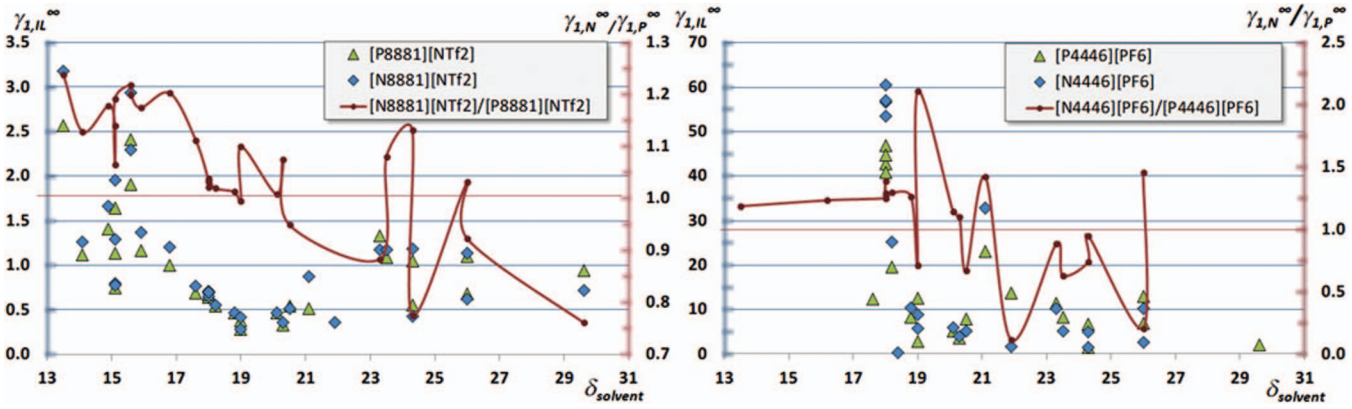

FIG. 4. Activity coefficients at infinite dilution as function of solvents solubility parameters. The solid curves are guides for the eyes.

determination of the ion pairs geometries and atom charges allows the evaluation of the impact of the cation's central atom on the IL structure, interactions capability and ultimately on the properties. Electrostatic potential-derived CHelpG charges calculations were conducted for the pairs $[N_{8,8,8,1}][NTf_2]/[P_{8,8,8,1}][NTf_2]$, $[N_{8,8,8,1}][PF_6]/[P_{8,8,8,1}][PF_6]$, and $[N_{4,4,4,6}][NTf_2]/[P_{4,4,4,6}][NTf_2]$; coordinates and Mulliken and CHelpG charges for all atoms are given as supplementary material.[43] While Mulliken charges are based on orbital occupancies, CHelpG electrostatic potential-derived charges allocate point charges to fit the computed electrostatic potential at a number of points at the molecular *van der Waals* surface.

With respect to the CHelpG electrostatic potential-derived charges, the **P** atom of the respective phosphonium-based cations has a positive partial charge ($[P_{8,8,8,1}][NTf_2]$: +0.306; $[P_{4,4,4,6}][NTf_2]$: +0.318 and $[P_{8,8,8,1}][PF_6]$: +0.404) while the **N** atom in the ammonium-based cations is nearly electro-neutral, ($[N_{8,8,8,1}][NTf_2]$: −0.078; $[N_{4,4,4,6}][NTf_2]$: +0.111 and $[N_{8,8,8,1}][PF_6]$: −0.042) due to a noticeable charge delocalization occurring in the alkyl ammonium cations, when compared with the respective phosphonium congeners. The CHelpG charge partitioning across the cationic carbon backbone is not uniform with symmetry; averaging electrostatic charges over all significant ion pair conformers calculated by the DFT/CHelpG method should yield a more accurate picture, but this approach was beyond the scope of this work.

Furthermore, partial atomic charges were retrieved from Natural Population Analysis (NPA). The most important results are summarized in Figure 5; further information is given in the supplementary material;[43] the results do support the CHelpG results with respect to the center atoms. The NPA partial charges assigned for the carbon and hydrogen atoms of the methylene groups adjacent to the center atom are distinctively different of the ones encountered in alkanes (e.g., inside an octane carbon chain, calculated at the same level of theory): the hydrogen atoms are more positive in all cases, while the carbon atoms are less negatively charged in the **N** ILs and more negatively charged in the **P** ILs. The found charges at the center atoms are significantly different: e.g., in the exemplary case of the pair $[N_{4,4,4,6}][NTf_2]/[P_{4,4,4,6}][NTf_2]$: −0.159 (**N**) and +1.491 (**P**). The adjacent methylene groups also are differently charged: +0.240 (**N**) and −0.180 (**P**). The methylene groups connected to **N** are in all cases more positively charged than in the case of **P**. Counting together the center charge and the charges of the adjacent methylene groups, one reaches to a slightly different net charge of the cationic center surrounded by four methylene groups: +0.800 (**N**) and +0.773 (**P**), indicating slightly stronger Coulomb-interactions in the respective ammonium cationic center. Within this perimeter, while having nearly the same net charge, the positive charge is more evenly distributed in the **N** species (reflecting hybridization), while it concentrates at the center in the case of **P**. Only after reaching a distance of three **C** atoms from the respective center atoms, similar charges are assigned like in octane,

TABLE V. EC_{50} values estimated for 5, 15, and 30 min of exposure to the luminescent marine bacteria *Vibrio fischeri*.

	EC_{50} (mg l^{-1}) – confidence bound (lower; upper)		
Ionic liquid	5 min	15 min	30 min
$[P_{4,4,4,6}][NTf_2]$	4.30 (3.78; 4.81)	3.83 (2.85; 4.81)	6.55 (4.28; 8.83)
$[N_{4,4,4,6}][NTf_2]$	18.19 (16.41; 19.98)	15.55 (14.67; 16.42)	17.80 (14.30; 21.30)
$[P_{4,4,4,6}][PF_6]$	45.64 (41.38; 49.90)	42.15 (37.78; 46.53)	42.95 (26.43; 59.46)
$[N_{4,4,4,6}][PF_6]$	78.27 (68.53; 88.01)	61.27 (51.77; 70.77)	63.35 (54.28; 72.42)
$[P_{8,8,8,1}][NTf_2]$			4.37 (0.00; 17.50)
$[N_{8,8,8,1}][NTf_2]$			23.30 (19.88; 26.72)
$[P_{4,4,4,4}][PF_6]$	192.79 (62.28; 323.30)	118.24 (49.99; 186.48)	106.77 (39.68; 173.86)
$[N_{4,4,4,4}][PF_6]$		270.60 (253.14; 306.06)	200.07 (185.20; 214.94)

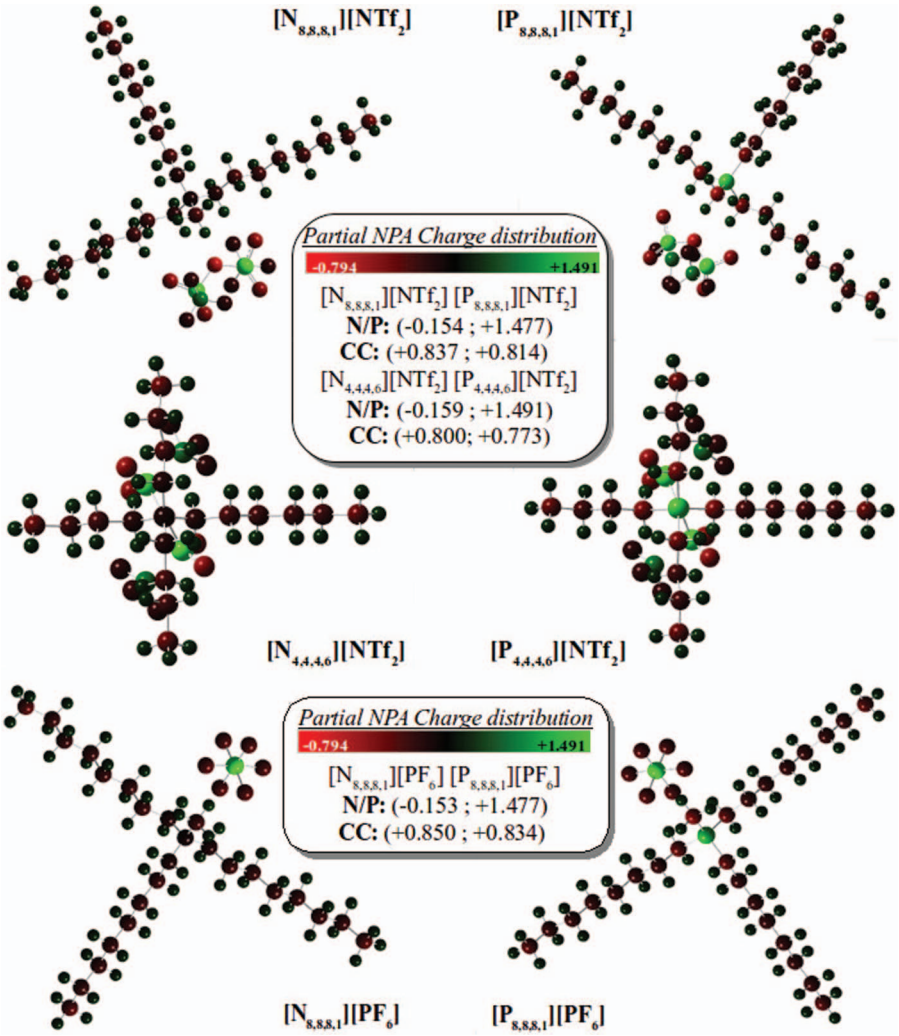

FIG. 5. Partial NPA charge distribution details for the studied ILs, retrieved at the BP-TZVP level of theory, for a fixed charge range. Charges of the central atoms (**N** or **P**) and cationic centers (CC, comprising the respective central atom and adjacent methylene/methyl groups) are presented. Complete pictures are given in the supplementary material.[43]

for both IL families. These results suggest that, while the **P** atom on the phosphonium cations is more charged than the **N** at the ammonium, since they are shielded by the tetragonal disposition of the alkyl chains a direct interaction with the central atom will be unlikely. The charge delocalization at the ammonium makes thus the central part of these cations more charged, and thus more polar, than at the corresponding phosphonium. Furthermore the polarizabilities obtained through the quantum chemical gas phase calculations, at the BP/TZVP level, are in good agreement with the experimental ones as shown in Table III.

Recently Castner and co-workers[14] investigated the cation-anion interactions, exploring the proximities between ions, for two pairs of isoelectronic ILs using nuclear overhauser effect 2D NMR methods. The authors observed significant differences in the nuclear dipolar interactions between the octyl-substituted N_{2228}^+/NTf_2^- and P_{2228}^+/NTf_2^-, with the NTf_2 anions concentrated heavily around the head group of the N_{2228}, leaving the rest of the cation almost free of interactions with the NTf_2 anions, while for the P_{2228} cation, the NTf_2 anion interacts with the middle and terminal hydrogens of the cation alkyl chain. Both the quantum chemical gas phase calculations as the Castner *et al.*[14] NMR studies support the effect of the cation's central atom change on the ILs properties.

If one pictures the ammonium-based ILs as having a stronger cation-anion interaction due to the charge delocalization than the phosphonium-based ILs that present the anion positioned around the cation alkyl chains, the increase of the density and viscosity can be seen as direct consequences of this arrangement, as well as the increased free volume of the phosphonium that is estimated from the refractive index measurements. Furthermore the charge delocalization also confers a higher polarity to the ammonium cation, in opposition to the more concentrated but not accessible charge of the phosphonium cation. This would explain the higher activity coefficients at infinite dilution for non-polar solvents, decreasing until becoming slightly lower for polar solvents, observed for the ammonium ILs. Finally, the ammonium rigid structure will also lead to a more compact bulk structure and therefore to, as shown in Table II, higher melting temperatures and lower melting entropies since the entropy of the

solid phase will be lower than those of the corresponding phosphonium.

CONCLUSIONS

Aiming at understanding the ILs behavior in different environments and ultimately develop correlations, methods or heuristics to design task-specific ILs, a set of works have been conducted by us over the past years. In spite of the large number of works describing ILs as "*designer solvents*" the studies investigating their structural design are scarce. Here the influence of the ammonium- and phosphonium-based IL cation's central atom was investigated through the measurement of densities, viscosities, melting temperatures, refractive indices, activity coefficients at infinite dilution, and toxicities, against *Vibrio fischeri*, of pairs of ammonium- and phosphonium-based ILs.

Although a shielding effect due to the surrounding cation's alkyl chains was expected, smoothing or even removing the influence of the cation's central atom on the interactions, structure or ultimately on the properties, what the density, viscosity, melting temperatures, refractive indices, infinite dilution activity coefficients, and toxicity results show is the opposite. In fact, all the properties investigated are pronouncedly affected by the cation central atom nature.

Geometries and atom charges of the isolated ion pairs were calculated using the TZVP basis set and non-local BP exchange/correlation function. The results show a greater charge delocalization near the cation central atom that induces a stronger cation anion interaction for the ammonium-based ILs. Furthermore, the differences in the nuclear dipolar interactions between the octyl-substituted $N_{2228}{}^{+}/NTf_2{}^{-}$ and $P_{2228}{}^{+}/NTf_2{}^{-}$ observed by Caster and co-workers allow us to picture the ammonium-based ILs with a more rigid structure, with the cation preferentially around the head group of the cation, and therefore with higher densities, viscosities, and melting temperatures than the phosphonium ILs, that present a more movable anion that interacts either with the cation head group or with the cation's alkyl chain terminal hydrogen. This less rigid structure confers the phosphonium ILs with higher free volume and polarizability. Furthermore, the NTf_2 anions concentrated heavily around the head group of the ammonium-based ILs, leaving the rest of the cation almost free of the NTf_2 anions, explains their higher activity coefficients at infinite dilution for non-polar solvents, decreasing until becoming slightly lower for polar solvents.

ACKNOWLEDGMENTS

The authors acknowledge the financial support from FCT – *Fundação para a Ciência e a Tecnologia* through the projects PTDC/QUI-QUI/121520/2010, PTDC/AAC-AMB/119172/2010, and Pest-C/CTM/LA0011/2013 and Ph.D. Grant SFRH/BD/74551/2010 of M.L.S.B. and post-doctoral Grants SFRH/BPD/38637/2007, SFRH/BPD/82264/2011, and SFRH/BPD/79263/2011 of B.S., P.J.C. and S.P.M.V., respectively.

[1]M. J. Earle and K. R. Seddon, Pure Appl. Chem. **72**, 1391 (2000).
[2]K. R. Seddon, Nat. Mater. **2**, 363 (2003).
[3]M. J. Earle, J. M. S. S. Esperanca, M. A. Gilea, J. N. Canongia Lopes, L. P. N. Rebelo, J. W. Magee, K. R. Seddon, and J. A. Widegren, Nature (London) **439**, 831 (2006).
[4]M. G. Freire, C. M. S. S. Neves, K. Shimizu, C. E. S. Bernardes, I. M. Marrucho, J. A. P. Coutinho, J. N. Canongia Lopes, and L. P. N. Rebelo, J. Phys. Chem. B **114**, 15925 (2010).
[5]M. A. A. Rocha, C. F. R. A. C. Lima, L. R. Gomes, B. Schröder, J. A. P. Coutinho, I. M. Marrucho, J. M. S. S. Esperança, L. P. N. Rebelo, K. Shimizu, J. N. C. Lopes, and L. M. N. B. F. Santos, J. Phys. Chem. B **115**, 10919 (2011).
[6]M. A. A. Rocha, J. A. P. Coutinho, and L. M. N. B. F. Santos, J. Phys. Chem. B **116**, 10922 (2012).
[7]S. M. Ventura, A. M. Gonçalves, T. Sintra, J. Pereira, F. Gonçalves, and J. P. Coutinho, Ecotoxicology **22**, 1 (2013).
[8]K. Tsunashima and M. Sugiya, Electrochem. Commun. **9**, 2353 (2007).
[9]K. Tsunashima, E. Niwa, S. Kodama, M. Sugiya, and Y. Ono, J. Phys. Chem. B **113**, 15870 (2009).
[10]H. Shirota, H. Fukazawa, T. Fujisawa, and J. F. Wishart, J. Phys. Chem. B **114**, 9400 (2010).
[11]H. Shirota and E. W. Castner, J. Phys. Chem. B **109**, 21576 (2005).
[12]H. Shirota, K. Nishikawa, and T. Ishida, J. Phys. Chem. B **113**, 9831 (2009).
[13]S. Seki, K. Hayamizu, S. Tsuzuki, K. Fujii, Y. Umebayashi, T. Mitsugi, T. Kobayashi, Y. Ohno, Y. Kobayashi, Y. Mita, H. Miyashiro, and S. Ishiguro, Phys. Chem. Chem. Phys. **11**, 3509 (2009).
[14]H. Y. Lee, H. Shirota, and E. W. Castner, J. Phys. Chem. Lett. **4**, 1477 (2013).
[15]P. J. Carvalho, T. Regueira, L. M. N. B. F. Santos, J. Fernandez, and J. A. P. Coutinho, J. Chem. Eng. Data **55**, 645 (2010).
[16]X. Paredes, O. Fandiño, M. J. P. Comuñas, A. S. Pensado, and J. Fernández, J. Chem. Thermodyn. **41**, 1007 (2009).
[17]J. N. Israelachvili, *Intermolecular and Surface Forces* (Academic Press, San Diego, 2011).
[18]A. R. H. Goodwin, K. N. Marsh, and W. A. Wakeham, *Measurement of the Thermodynamic Properties of Single Phases*, IUPAC Experimental Thermodynamics Vol. VI (Elsevier, Amsterdam, 2003), pp. 435–451.
[19]P. Brocos, Á. Piñeiro, R. Bravo, and A. Amigo, Phys. Chem. Chem. Phys. **5**, 550 (2003).
[20]A. J. B. Cruickshank, M. L. Windsor, and C. L. Young, Proc. R. Soc. London, Ser. A **295**, 259 (1966).
[21]A. J. B. Cruickshank, M. L. Windsor, and C. L. Young, Proc. R. Soc. London, Ser. A **295**, 271 (1966).
[22]A.-L. Revelli, L. M. Sprunger, J. Gibbs, W. E. Acree, G. A. Baker, and F. Mutelet, J. Chem. Eng. Data **54**, 977 (2009).
[23]MicrotoxOmni® 4.1 Strategic Diagnostics Inc., SDI 2009, Newark, NJ, U.S.A.
[24]S. P. M. Ventura, C. S. Marques, A. A. Rosatella, C. A. M. Afonso, F. Gonçalves, and J. A. P. Coutinho, Ecotoxicol. Environ. Saf. **76**, 162 (2012).
[25]AZUR Environmental, MicrotoxOmni™ Software for Windows(r) 95/98/NT. 1999, Carlsbad, CA, U.S.A.
[26]M. J. Frisch, G. W. Trucks, H. B. Schlegel, G. E. Scuseria, M. A. Robb, J. R. Cheeseman, J. A. Montgomery, Jr., T. Vreven, K. N. Kudin, J. C. Burant, J. M. Millam, S. S. Iyengar, J. Tomasi, V. Barone, B. Mennucci, M. Cossi, G. Scalmani, N. Rega, G. A. Petersson, H. Nakatsuji, M. Hada, M. Ehara, K. Toyota, R. Fukuda, J. Hasegawa, M. Ishida, T. Nakajima, Y. Honda, O. Kitao, H. Nakai, M. Klene, X. Li, J. E. Knox, H. P. Hratchian, J. B. Cross, V. Bakken, C. Adamo, J. Jaramillo, R. Gomperts, R. E. Stratmann, O. Yazyev, A. J. Austin, R. Cammi, C. Pomelli, J. W. Ochterski, P. Y. Ayala, K. Morokuma, G. A. Voth, P. Salvador, J. J. Dannenberg, V. G. Zakrzewski, S. Dapprich, A. D. Daniels, M. C. Strain, O. Farkas, D. K. Malick, A. D. Rabuck, K. Raghavachari, J. B. Foresman, J. V. Ortiz, Q. Cui, A. G. Baboul, S. Clifford, J. Cioslowski, B. B. Stefanov, G. Liu, A. Liashenko, P. Piskorz, I. Komaromi, R. L. Martin, D. J. Fox, T. Keith, M. A. Al-Laham, C. Y. Peng, A. Nanayakkara, M. Challacombe, P. M. W. Gill, B. Johnson, W. Chen, M. W. Wong, C. Gonzalez, and J. A. Pople, Gaussian 03, Revision D.02, Wallingford, CT, 2004.
[27]R. S. Mulliken, J. Chem. Phys. **36**, 3428 (1962).
[28]C. M. Breneman and K. B. Wiberg, J. Comp. Chem. **11**, 361 (1990).
[29]C. M. S. S. Neves, A. R. Rodrigues, K. A. Kurnia, J. M. S. S. Esperança, M. G. Freire, and J. A. P. Coutinho, Fluid Phase Equilib. **358**, 50 (2013).
[30]S. Seki, S. Tsuzuki, K. Hayamizu, Y. Umebayashi, N. Serizawa, K. Takei, and H. Miyashiro, J. Chem. Eng. Data **57**, 2211 (2012).
[31]A. F. M. Barton, *Handbook of Solubility Parameters and Other Cohesion Parameters*, 2nd ed. (CRC Press, 1991).

[32]M. L. S. Batista, C. M. S. S. Neves, P. J. Carvalho, R. Gani, and J. A. P. Coutinho, J. Phys. Chem. B **115**, 12879 (2011).
[33]M. A. Pena, Y. Daali, J. Barra, and P. Bustamante, Chem. Pharm. Bull. (Tokyo) **48**, 179 (2000).
[34]P. Bustamante, R. Ochoa, A. Reillo, and J.-B. Escalera, Chem. Pharm. Bull. (Tokyo) **42**, 1129 (1994).
[35]A. Jouyban-Gharamaleki, S. Romero, P. Bustamante, and B. J. Clark, Chem. Pharm. Bull. (Tokyo) **48**, 175 (2000).
[36]S. Romero, A. Reillo, B. B. Escalera, and P. Bustamante, Chem. Pharm. Bull. (Tokyo) **44**, 1061 (1996).
[37]K. Tumba, T. Letcher, P. Naidoo, and D. Ramjugernath, J. Chem. Thermodyn. **49**, 46 (2012).
[38]P. Reddy, N. V. Gwala, N. Deenadayalu, and D. Ramjugernath, J. Chem. Thermodyn. **43**, 754 (2011).
[39]S. Stolte, S. Steudte, O. Areitioaurtena, F. Pagano, J. Thöming, P. Stepnowski, and A. Igartua, Chemosphere **89**, 1135 (2012).
[40]D. J. Couling, R. J. Bernot, K. M. Docherty, J. K. Dixon, and E. J. Maginn, Green Chem. **8**, 82 (2006).
[41]M. Matzke, J. Arning, J. Ranke, B. Jastorff, and S. Stolte, *Design of Inherently Safer Ionic Liquids: Toxicology and Biodegradation* (Wiley-VCH Verlag GmbH & Co, 2010).
[42]J. Ranke, A. Müller, U. Bottin-Weber, F. Stock, S. Stolte, J. Arning, R. Störmann, and B. Jastorff, Ecotoxicol. Environ. Saf. **67**, 430 (2007).
[43]See supplementary material at http://dx.doi.org/10.1063/1.4864182 for atom coordinates and charges from Mulliken population analysis, Natural Population Analysis (NPA), and electrostatic potential-derived (CHelpG) charges, calculated at the BP-TZVP level of theory for the ILs studied.